Assessment of the NCEP–DOE Reanalysis-2 and TOVS Pathfinder A Moisture Fields and Their Use in Antarctic Net Precipitation Estimates

CHENG-ZHI ZOU

Office of Research and Applications, NOAA/NESDIS, and Joint Center for Satellite Data Assimilation, Camp Springs, Maryland

MICHAEL L. VAN WOERT

Office of Research and Applications, NOAA/NESDIS, Camp Springs, Maryland, and U.S. National Ice Center, Washington, D.C.

CHUANYU XU

U.S. National Ice Center, Washington, D.C., and QSS Group, Inc., Lanham, Maryland

KAMRAN SYED

Cooperative Institute for Climate Studies, University of Maryland, College Park, Maryland

(Manuscript received 7 May 2003, in final form 23 April 2004)

ABSTRACT

Moisture fields from the NCEP–DOE reanalysis-2 (R-2) and Television Infrared Observational Satellite (TIROS) Operational Vertical Sounder (TOVS) Pathfinder A are validated using the Special Sensor Microwave Imager (SSM/I) retrievals over the Southern Ocean. It is shown that the spatial distributions of the annual mean statistics of the total precipitable water are similar among SSM/I, R-2, and TOVS Pathfinder A for both the eddy and mean components. However, transient statistics show that the R-2 total precipitable water agrees with SSM/I with a correlation of 0.77 over the Southern Ocean while the TOVS Pathfinder A moisture is almost uncorrelated with the SSM/I data.

Total moisture transport convergence for 1988 over the Antarctic continent is further examined using the R-2 wind and moisture data as well as the moisture retrievals from TOVS Pathfinder A. To gain a better understanding of transient and mean processes on moisture transport, the total moisture transport was decomposed into mean and eddy components. The results suggest that a mass conservation correction is necessary for the mean component, but can safely be ignored for the eddy component. With the mass conservation correction, the mean moisture transport is about the same for both the R-2 estimate alone and the estimate based on the mixed TOVS Pathfinder A moisture–R-2 wind. The computed eddy and total moisture transport convergence over Antarctica for the R-2 data agrees within 10%–15% with previous surface-data-based estimates as well as estimates from other model analyses. However, the eddy component of the mixed TOVS moisture with R-2 wind is about 60%–70% lower than the R-2 result. These differences occur because the eddy moisture amplitude of the TOVS Pathfinder A is nearly 40% lower than the R-2 data and also because the TOVS moisture has a much lower correlation with the R-2 winds. These results reflect the difficulties with the TOVS sensor in quantifying synoptic moisture transients resulting from conditional sampling problems.

1. Introduction

Moisture transport as well as its convergence over the polar region has been recognized as an important component in global climate change scenarios. The variation of the polar moisture convergence is closely related to variations in the sea ice and polar ice cap through direct snowfall accumulation. The snowfall changes the surface albedo and thus the surface energy balance, which in turn interacts with the atmosphere and thus affects the atmospheric general circulation. The moisture transport also directly influences atmospheric heating by changing the cloud condensation amount and the cloud cover, which changes the atmospheric albedo, and thus the atmospheric absorption and emission of both the terrestrial and solar radiation.

Three kinds of datasets have been used to quantitatively estimate the high-latitude moisture convergence and its variation: radiosonde observations of wind and moisture profiles (e.g., Peixóto and Oort 1983; Bromwich 1988; Connolley and King 1993; Serreze et al.

Corresponding author address: Dr. Cheng-Zhi Zou, Office of Research and Applications, NOAA/NESDIS, NOAA Science Center, Room 712, 5200 Auth Road, Camp Springs, MD 20746.
E-mail: Cheng-Zhi.Zou@noaa.gov

1995), analyses/reanalyses data (e.g., Bromwich et al. 1995; Giovinetto et al. 1997; Cullather et al. 1996, 1998, 2000; Genthon and Krinner 1998), and satellite-retrieved datasets (Slonaker and Van Woert 1999; Zou and Van Woert 2001; Groves and Francis 2002a,b). Of the three kinds of datasets, greater efforts have been devoted to using the model analysis and reanalysis data in moisture convergence studies. This is because these analyses have the advantage that they include various routine observations from satellites, ships, buoys, aircraft, and the radiosonde network, etc., combined with analysis/forecast models that contain a comprehensive set of physical parameterizations. They are also easy to use since they are in gridded formats with global coverage for extended time periods.

The polar moisture convergence studies are further divided into the Arctic and Antarctic regions. Bromwich et al. (1995), Giovinetto et al. (1997), Cullather et al. (1996, 1998), and Genthon and Krinner (1998) performed comprehensive studies of the Antarctic moisture budget and its long-term variation using various model analyses and reanalyses. Cullather et al. (2000) and Rogers et al. (2001) investigated the Arctic moisture convergence and its temporal variation using European Centre for Medium-Range Weather Forecasts (ECMWF) and National Centers for Environmental Prediction–National Center for Atmospheric Research (NCEP–NCAR) reanalyses. Cullather et al.'s (2000) study suggests that over the Arctic region, the long-term and area-averaged net precipitation estimated from the ECMWF and NCEP–NCAR reanalyses agree within 10%. For instance, the total net precipitation for the period 1979–93 over the 70°–90°N region is 182 mm yr^{-1} for the ECMWF reanalyses and 194 mm yr^{-1} for the NCEP–NCAR reanalyses, respectively. However, their study also shows that these numbers are significantly different (up to 30% to 60%) from the results using the ECMWF and NCEP–NCAR forecast fields, suggesting the significant impact of assimilation of the satellite and radiosonde data on the two reanalyses systems. In addition, the reanalyses results are about 10% to 20% higher than the radiosonde estimate of 163 mm yr^{-1} (Serreze et al. 1995).

Groves and Francis (2002a) argue that inaccurate reanalysis moisture fields may be responsible for the higher reanalysis estimates compared to radiosonde data. When they used satellite-retrieved moisture data, the so-called Television Infrared Observational Satellite (TIROS) Operational Vertical Sounder-Polar Pathfinder (TOVS Path-P; Francis 1994) products, combined with the NCEP–NCAR reanalysis winds, the total net precipitation poleward of 70°N was 151 mm yr^{-1}, a 23% reduction from the NCEP–NCAR reanalysis estimates. This number is closer to the radiosonde estimates, but on the low side. Local differences between the reanalyses and the mixed method of TOVS moisture–reanalyses wind tend to be even larger (Cullather et al. 2000; Rogers et al. 2001; Groves and Francis 2002a,b).

Over Antarctica, the differences in net precipitation estimates between different analyses and reanalyses are much larger than over the Arctic region. For instance, the multiyear NCEP–NCAR reanalysis precipitation over Antarctica reaches 335 mm yr^{-1} (Cullather et al. 1998). Bromwich et al. (1995) show that the Antarctic annual mean net precipitation calculated by the ECMWF, National Meteorological Center (NMC), and Australian Bureau of Meteorology (ABM) operational model analyses ranged from 89 to 157 mm yr^{-1} for the period 1985–92. In those studies, the ECMWF analysis and reanalysis estimates (Bromwich et al. 1995; Giovinetto et al. 1997; Genthon and Krinner 1998) appear to be closest to the snow stake estimates of 143–166 mm yr^{-1} (Giovinetto and Bentley 1985; Vaughan et al. 1999). However, it is a matter of ongoing debate as to the relative merits of using analysis versus reanalysis products in the study of the Antarctic net precipitation variability. This is because, on one hand, analysis products may produce spurious climate signals owing to frequent model updates in the system (Kalnay et al. 1996). On the other hand, however, coding mistakes have been found in both the ECMWF (Bromwich et al. 2000) and NCEP–NCAR (Kanamitsu et al. 2002) reanalyses over the Southern Ocean and Antarctica. These coding mistakes have caused large errors in some of the reanalysis variables. For instance, a height error in the assimilation of the Vostok station on the Antarctic continent caused large errors in the wind field of the ECMWF reanalysis (Bromwich et al. 2000). As a result, large discrepancies exist in the Antarctic net precipitation variability. Specifically, Cullather et al. (1996) showed close correspondence between the Southern Oscillation index (SOI) and the Antarctic net precipitation computed from the ECMWF operational analyses. In contrast, Genthon and Krinner (1998) found no convincing correlation between the SOI and Antarctic net precipitation based on the ECMWF reanalysis product.

In an effort to better estimate the Antarctic net precipitation, this study examines moisture and wind fields from the newly released NCEP–DOE reanalysis-2 (hereafter referred to as R-2; Kanamitsu et al. 2002). In addition, Groves and Francis (2002a) recently proposed a mixed method based on TOVS moisture fields and wind fields from numerical analyses over the Arctic Ocean. The soundness of this approach for Antarctic moisture budget studies will also be examined by combining moisture retrievals from the TOVS Pathfinder A (Susskind et al. 1997) and the wind fields from the R-2. Specifically, this study first assesses accuracy of the moisture fields from R-2 and TOVS Path A by comparing them with Special Sensor Microwave Imager (SSM/I) retrievals. Then the Antarctic net precipitation using the R-2 wind and moisture products and a mixed R-2 winds–TOVS Path A moisture product is investigated. The net precipitation results are compared to snow stake observations and previous estimates based on the ECMWF analysis. This provides a further as-

sessment of the R-2 and TOVS Path A moisture products. An understanding of these questions provides a foundation for the future use of these datasets in long-term trend and variability studies on the Antarctic moisture budget.

Section 2 introduces and validates the TOVS Pathfinder A and R-2 moisture products as well as the R-2 wind data. Section 3 describes the methodology used to estimate the Antarctic net precipitation. Section 4 presents the Antarctic net precipitation results. Section 5 is a summary.

2. Data

a. SSM/I total precipitable water

As part of the National Aeronautics and Space Administration (NASA) Pathfinder Program, Remote Sensing Systems has generated the SSM/I data products from July 1987 to the present using a unified, physically based algorithm (Wentz 1997). This algorithm simultaneously retrieves ocean wind speed, total precipitable water (TPW), cloud liquid water, and rain rate. The algorithm used for the retrievals has been carefully calibrated using an in situ database containing 37 650 SSM/I overpasses of buoys and 35 108 overpasses of radiosonde observations. The radiosonde observations were selected from 55 radiosonde sites that cover the global ocean. More than 10 radiosonde sites were located over the Arctic and Southern Oceans. The retrieved TPW has a root-mean-square (rms) error of 1.2 mm and a bias of 0.6 mm when validated using the 35 108 radiosonde observations. Because of this high accuracy and also because the SSM/I data were not used in the R-2 data assimilation system (Kanamitsu et al. 2002), the SSM/I TPW provides a reliable independent source of data for validating the R-2 and TOVS Path A data used in this study. The SSM/I data are available in several different formats. The daily orbital data, mapped to a 0.25° latitude × 0.25° longitude grid, are used in this study.

b. TOVS Pathfinder A moisture

The TOVS Pathfinder A dataset (Susskind et al. 1997) is based on the interactive physical retrieval scheme of the Goddard Laboratory for Atmosphere (GLA). In this system, the retrieval subsystem depends on the first-guess field, which is provided by the 6-h forecast of the GLA general circulation model. The retrieved satellite soundings, as well as other concurrent in situ measurements, are in turn used to create the initialization field for the next 6-h forecast. Susskind and Pfaendtner (1989) showed a large positive improvement in forecast skill (and thus also the first-guess field) using this interactive forecast–retrieval–assimilation system compared to those using operationally produced satellite soundings. In this study, the retrieved daily, layer precipitable water from TOVS Path A is used. This dataset has five layers: surface–850, 850–700, 700–500, 500–300, and 300–100 hPa. Susskind et al. (1997) validated this moisture field against radiosonde observations, SSM/I retrievals, and ECMWF reanalyses in a global and monthly mean sense. However, they did not specifically address the accuracy of the retrievals at high southern latitudes. In order to better understand the suitability of this dataset for net precipitation studies over Antarctica and Southern Ocean, here we compare the TOVS Pathfinder A TPW to SSM/I TPW over the Southern Ocean. In this study we also place a focus on daily statistics.

Temporal and spatial interpolation of the satellite data onto a common space–time grid needs to be performed before they can be used for comparisons and/or for moisture transport computations. The TOVS Path A and SSM/I data are provided in separate ascending and descending files. The TOVS Path A data have a grid resolution of 1° latitude × 1° longitude while the SSM/I data have a resolution of 0.25° latitude × 0.25° longitude. For the temporal interpolation scheme, single ascending or descending orbital passes are binned to the nearest standard output time (i.e., within a ±3 h interval of 0000, 0600, 1200, or 1800 UTC). If more than one orbit of data is found in the 6-h period, those data are linearly interpolated to the standard output time. An area-mean interpolation scheme is then applied to convert the temporal-interpolated data to the spatial grid as needed. For TOVS, an area-mean conversion from 1° × 1° to 2.5° × 2.5° resolution is conducted to facilitate its combination with the R-2 winds for moisture transport computations. For SSM/I, a conversion from 0.25° × 0.25° to 1° × 1° is performed for comparison with the TOVS moisture fields and to 2.5° × 2.5° for comparison with the R-2 moisture field. In the moisture transport computation, the TOVS layer precipitable water is further converted to the specific humidity at the surface, 850, 700, 500, and 300 hPa using the integral relationship between the two quantities (e.g., Bromwich et al. 1995). The trapezoidal rule is used for the integration under the assumption that the specific humidity at 100 hPa is zero and the surface pressure is 1000 hPa.

Figure 1 shows a comparison of the TOVS Path A and SSM/I annually averaged TPW for 1988. For completeness, both the mean and eddy statistics are included in the comparisons. In this comparison, the annual averages of the satellite datasets include all available retrievals; thus the statistics are based on different size datasets. In particular, the SSM/I retrievals include all clear and cloudy conditions, except for the heavily precipitating situations, while the TOVS Path A retrievals include only clear and partially cloudy conditions (≤80% cloud cover; Susskind et al. 1997). From Figs. 1a, 1b, 1d , and 1e it is seen that the overall patterns between the TOVS Path A and SSM/I are similar for both the mean and eddy components. However, the difference of the mean fields (Fig. 1c) shows that in the

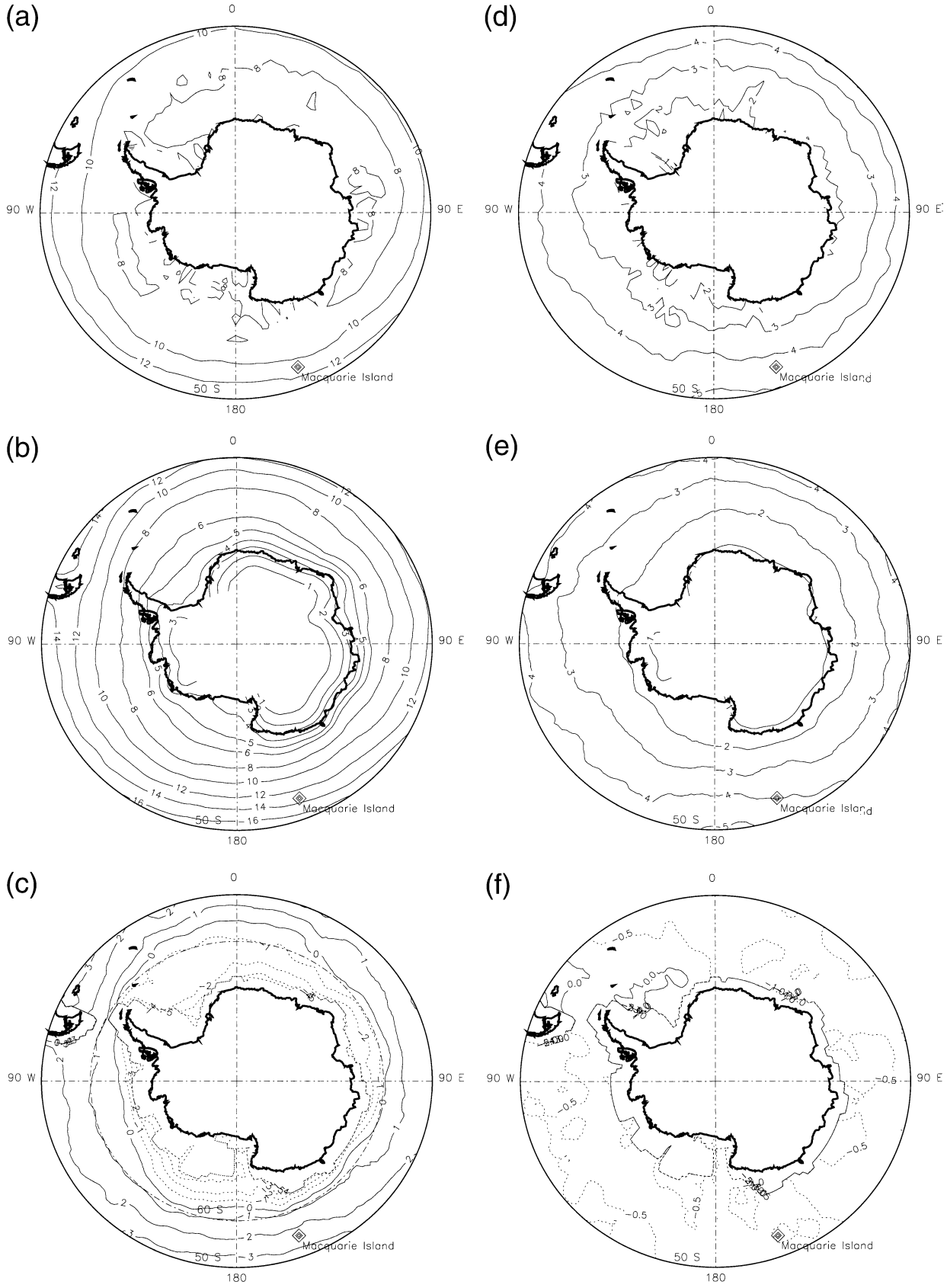

latitudinal belt 50°–60°S, the TOVS Path A TPW estimates are larger than the SSM/I estimates by 1 to 3 mm (corresponding to 10% to 20%). Poleward of 60°S the TOVS Path A TPW estimates are smaller than the SSM/I estimates. The maximum underestimation occurs close to the coastline of the Antarctic continent, especially near the Filchner–Ronne Ice Shelf where differences of up to 4 to 5 mm are found (corresponding to −40% to −50%). In contrast, the TOVS Path A eddy TPW is less than the SSM/I TPW by about −0.5 to −1 mm (−15% to −20%), and this difference is quite uniform over the whole Southern Ocean (Fig. 1f). Since the eddy TPW is small close to the coast of the Antarctic continent, the relative error near the coast can be as large as −30% to −40%.

To gain further insight into the TOVS Path A retrievals, Fig. 2 shows a scatterplot for 1988 of collocated TOVS Path A and SSM/I TPW on the 60°S latitudinal circle at intervals of 20° longitudes starting from 0°. Since this comparison contains only the collocated points, it does not incorporate cloudy regions of >80% because of limitations of the TOVS retrievals. For the data shown in Fig. 2, the annual mean TOVS Path A TPW is 8.0 mm and the SSM/I TPW is 8.2 mm, with a negligible bias of −0.2 mm. The rms error between the SSM/I and TOVS Path A TPW is 4.85 mm. The eddy TPW for TOVS and SSM/I are 3.5 and 3.7 mm, respectively, corresponding to a −4% difference. This result suggests that much of the difference observed in Fig. 1f (−0.5 to −1 mm or −10% to −15%) is caused by the missing TOVS moisture retrievals in overcast conditions.

The most striking feature of Fig. 2, however, is that, although the annually averaged mean and eddy statistics of the TOVS Path A and SSM/I are similar, their correlation is only ~0.1, suggesting that there are fundamental differences in the characteristics of the atmospheric observing system for the two satellites sensors. The scatterplots show a characteristic ''V'' shape, in which a moist (dry) atmosphere in the SSM/I data is associated with a dry (moist) atmosphere in the TOVS Path A data. Based on analyses by Stephens et al. (1994), the differences in the TOVS Path A and SSM/I TPW reflect different retrieval characteristics in convergent (lifting motion) and divergent (sinking) regions of the atmospheric baroclinic waves. Specifically, in sinking regions of the atmospheric baroclinic wave, where the surface temperature is relatively cold and large amounts of moisture exist in the middle troposphere, the TOVS retrieves excessive moisture. Conversely, in regions of atmospheric convergence, where large amount of moisture exist in the surface layer and the surface temperature is relatively warm, the TOVS retrievals are typically too dry. These regional differences in atmospheric dynamics and associated differences in the TOVS Path A moisture products will have a significant impact on the derived eddy moisture transport estimates.

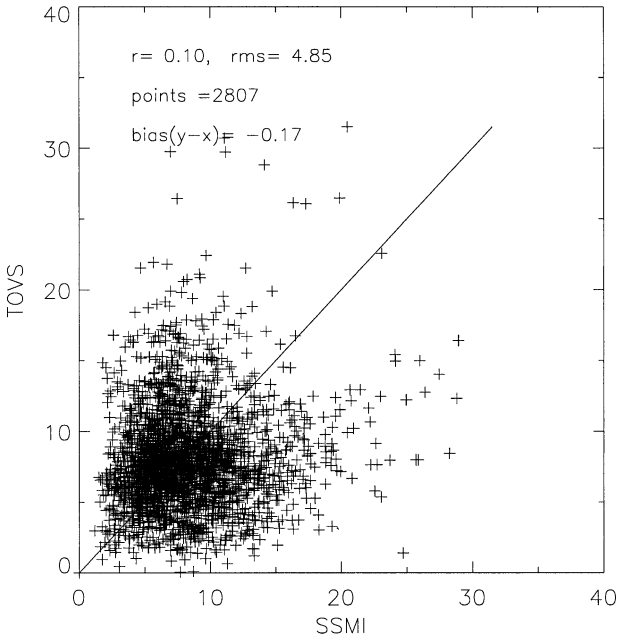

FIG. 2. Scatterplot of TPW between SSM/I and TOVS Path A on the 60°S lat circle in increments of 20° lon starting at 0°. Unit is mm.

c. NCEP–DOE reanalysis-2 moisture

The newly released R-2 dataset (Kanamitsu et al. 2002) is an update to the previous NCEP–NCAR reanalyses. The R-2 uses a state-of-the-art global spectral model with a triangular spectral resolution of T62 and 28 vertical levels in the analyses and forecasts. It has corrected many of the known problems found in the earlier NCEP–NCAR reanalyses. Some of the corrected problems specifically involve the Southern Hemisphere, such as the so-called PAOBS (Southern Hemisphere bogus data) problem where observations were shifted by 180° longitude for the period 1979–94 (Kanamitsu et al. 2002). Having corrected the coding errors in the NCEP–NCAR reanalyses and improved many aspects of the model physics (Kanamitsu et al. 2002), R-2 is expected to perform better than the NCEP–NCAR reanalyses over the Antarctic and subantarctic regions in an overall statistical sense. However, details on the improvement of specific fields can only be determined through a detailed analysis and independent validation. Since neither the SSM/I data

←

FIG. 1. TOVS Pathfinder A and SSM/I mean and eddy TPW comparisons for 1988: (a) SSM/I mean component; (b) TOVS Path A mean component; (c) [(b) − (a)]; (d) SSM/I eddy component; (e) TOVS Path A eddy component; and (f) [(e) − (d)]. Contour unit is mm.

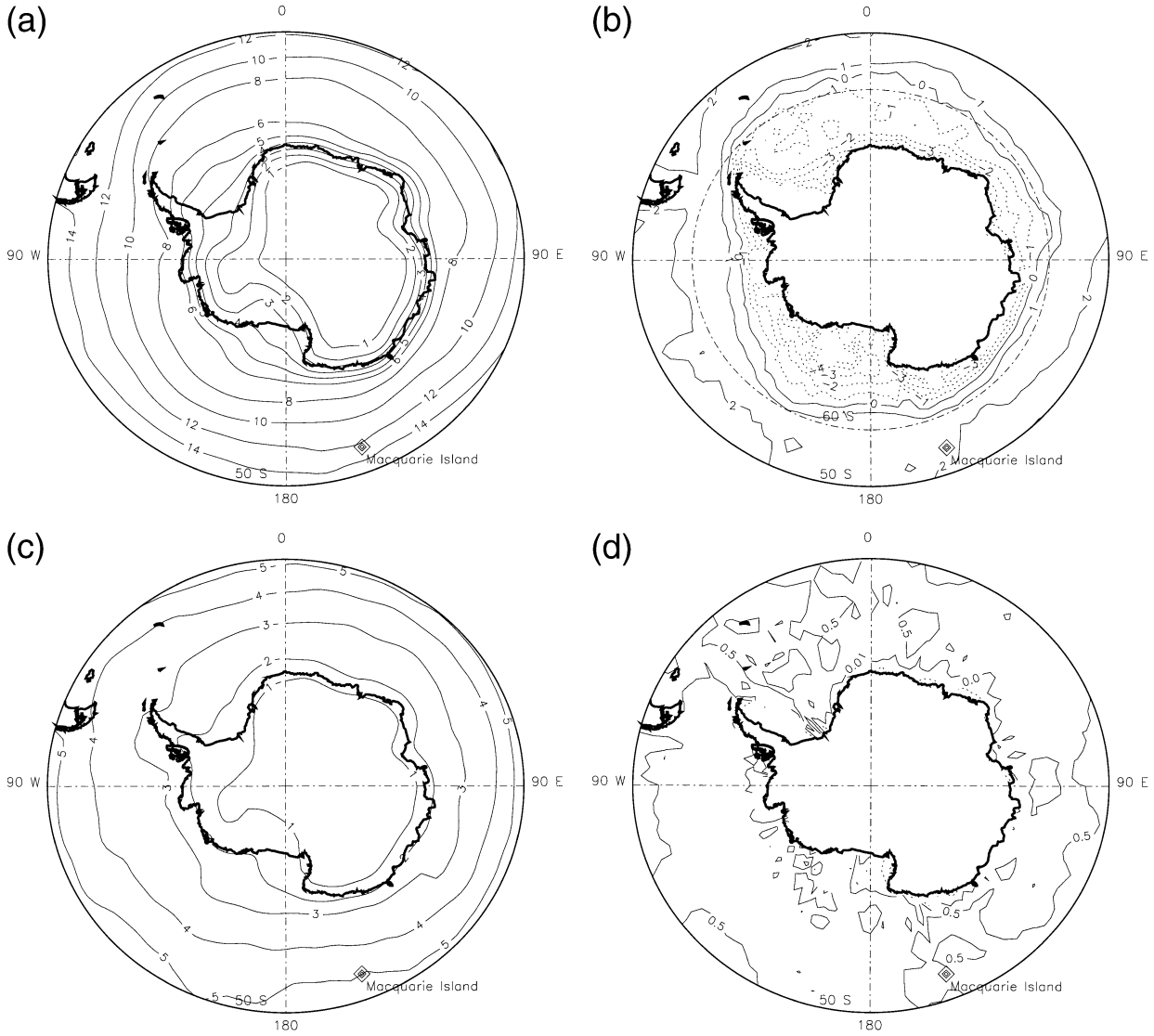

FIG. 3. The R-2 and SSM/I mean and eddy TPW comparisons for 1988: (a) R-2 mean component; (b) [(a) − (Fig. 1a)]; (c) R-2 eddy component; and (d) [(c) − (Fig. 1d)]. Contour unit is mm.

nor the TOVS moisture data are included in the R-2 (Kanamitsu et al. 2002), comparisons with these two datasets can provide a robust validation and understanding of the R-2 moisture field.

The 1988 annually averaged mean and eddy R-2 TPW as well as their differences with SSM/I are shown in Figs. 3a–d. For the mean component, the differences between the R-2 and SSM/I fields (Fig. 3b) are similar to the differences between TOVS Path A and SSM/I (Fig. 2c), suggesting that the mean component of R-2 TPW is similar to TOVS Path A. In contrast, except for a small area near Ross Ice Shelf, the R-2 eddy TPW overestimates SSM/I by about 0.5 mm (10% to 20%) over most of the Southern Ocean (Fig. 3d). Considering the combined effects of underestimation by the TOVS Path A and overestimation by the R-2, the eddy component of the TOVS Path A TPW is about 1 to 1.5 mm (30% to 40%) smaller than R-2 over most of the Southern Ocean.

Figure 4 shows a scatterplot for 1988 of collocated R-2 and SSM/I TPW on the 60°S latitudinal circle at intervals of 40° longitudes starting from 0°. In contrast to Fig. 2, which includes only the clear and partially cloudy sites, this plot contains all clear and cloudy conditions except for the heavily precipitating situations. In Fig. 4, the rms error between the R-2 and SSM/I TPW is 2.93 mm and their correlation is 0.77. The annual mean TPW is 9.5 mm for R-2 and 8.4 mm for SSM/I. Dividing by the SSM/I yearly mean TPW value, the relative rms error of R-2 is 35%, compared to a 60% relative rms error for TOVS Path A. In addition, the eddy TPW for R-2 is 4.2 and 3.6 mm for SSM/I, cor-

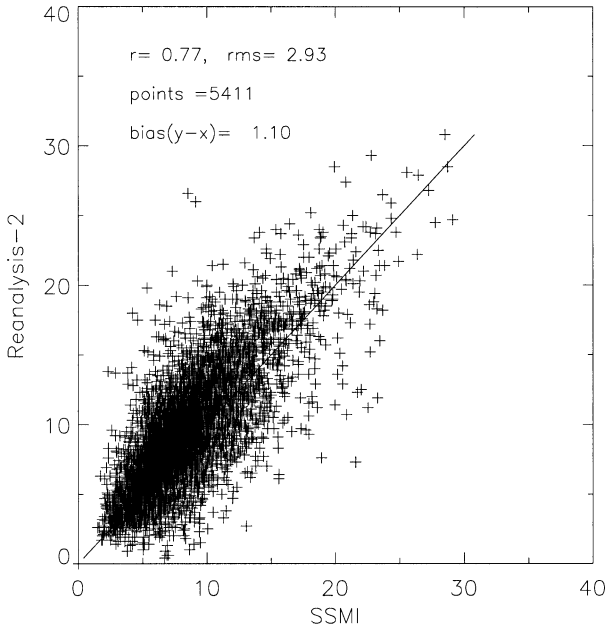

FIG. 4. Scatterplot of TPW for 1988 between SSM/I and R-2 on the 60°S lat circle at intervals of 40° lon starting from 0°. Unit is mm.

responding to a 0.6 mm (16%) difference. These results are consistent with Fig. 3d, suggesting that excluding the heavily precipitating conditions does not alter the statistical characteristics of the R-2 TPW. The large correlation and smaller rms errors between the R-2 and SSM/I TPW suggest that the R-2 moisture fields are of higher quality than the TOVS Path A moisture fields.

d. NCEP–DOE Reanalysis-2 winds

In this study, the R-2 wind profiles are combined with both the TOVS Path A and R-2 moisture fields to estimate the moisture convergence over the Antarctic continent. In order to understand the performance of the R-2 winds over the Southern Ocean and Antarctic region, we have compared the 1988 annually averaged R-2 mean and eddy atmospheric circulation statistics with the ECMWF analyses. Since the atmospheric circulation structure of the ECMWF analyses had been well analyzed by previous authors (e.g., Trenberth and Olson 1988), it can provide a reference for accessing the quality of the R-2 wind. Figures 5a and 5b show a comparison for 1988 of the annually averaged eddy statistics for the meridional wind, $\sqrt{\overline{v'^2}}$, on the 60°S latitudinal circle. The figures show that the patterns of the ECMWF analyses and R-2 eddy statistics of the meridional wind are very similar, though the amplitudes of the R-2 $\sqrt{\overline{v'^2}}$ are 5% to 10% lower than the ECMWF analyses. Similar comparisons have also been made for the eddy statistics of the zonal wind and the mean components of both the zonal and meridional winds (not shown). Overall, the annually averaged statistics suggest that the R-2 and ECMWF

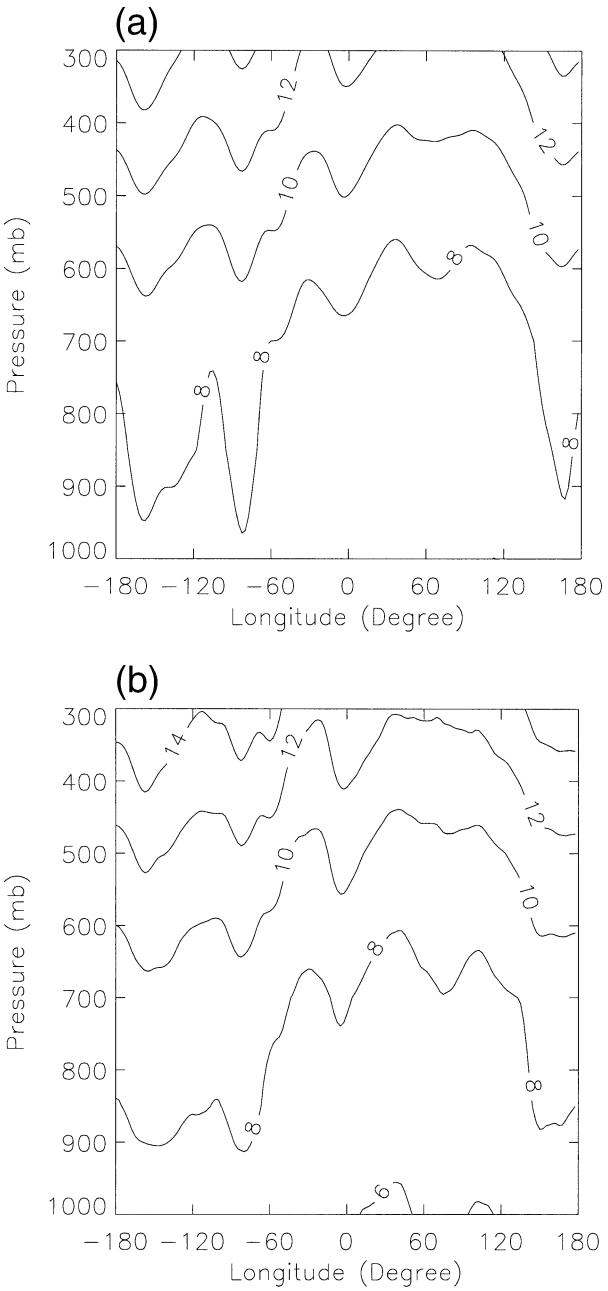

FIG. 5. The 1988 annual mean $\sqrt{\overline{v'^2}}$ at 60°S: (a) R-2, and (b) ECMWF analyses. Unit is m s^{-1}.

eddy and mean fields exhibit similar atmospheric circulation structure.

Despite the similarities in the statistical structure of the R-2 and ECMWF atmospheric circulation patterns, there is no guarantee that R-2 winds perform well over the Southern Ocean. Francis (2002) found that the ECMWF and NCEP–NCAR reanalyses upper-level winds exhibit large biases (up to 3 to 4 m s^{-1}) when validated against independent radiosonde observations over the Arctic Ocean. It is reasonable to suspect that

the R-2 wind may suffer similar problems over the Southern Ocean and Antarctica. Ideally, to have confidence in the accuracy of these data, an evaluation against independent observations must be conducted. Unfortunately, we are unaware of the existence of any independent radiosonde data over the Southern Ocean and Antarctica. Therefore, judgment of the performance of the R-2 winds in the Antarctic moisture budget studies can only be made after the computation is completed. Comparisons of the R-2 and ECMWF net precipitation results as well as the surface-based estimates that will be shown later suggest that the R-2 winds are reasonably accurate over the Southern Ocean.

3. Methodology

One of the goals of this study is to estimate the Antarctic net precipitation using the moisture budget equation with reanalyses and satellite data products as inputs. The atmospheric moisture budget equation in an isobaric coordinate system is written as

$$P - E = -\frac{\partial W}{\partial t} - \nabla \cdot \frac{1}{g} \int_0^{p_s} q\mathbf{V}\, dp, \qquad (1)$$

where P represents precipitation/snowfall, E surface evaporation/sublimation, W the precipitable water of a whole atmospheric column, q the specific humidity, $\mathbf{V}$ the horizontal wind vector, p_s the surface pressure, and g the gravity constant. The magnitude of the moisture storage term $\partial W/\partial t$ is usually much smaller than the moisture convergence for seasonal time scales and beyond (Peixóto and Oort 1992) and thus, it is ignored. Integrating (1) over the surface of the continent and divided by the area of the continent, S, gives the spatially averaged difference between precipitation and evaporation. Then using Gauss's divergence theorem, the moisture transport divergence over a specific region can be written as a closed line integral around the border of that region. Thus, the long-term, spartially averaged net precipitation can be expressed as

$$\langle \overline{P} \rangle - \langle \overline{E} \rangle = -\frac{1}{\overline{S}} \oint \left(\int_0^{p_s} \overline{\mathbf{V}q}\, \frac{dp}{g} \right) \cdot \mathbf{n}\, dl, \qquad (2)$$

where dl represents the line increment along the Antarctic border, and $\mathbf{n}$ represents the outward normal to the area perimeter. The overbar denotes monthly or annually averaged values, and the $\langle\ \rangle$ represent an area average. In the computation, the total moisture transport $\overline{\mathbf{V}q}$ in Eq. (2) is further split into the summation of the mean component, $\overline{\mathbf{V}}\,\overline{q}$, and eddy component, $\overline{\mathbf{V}'q'}$. In this study, monthly mean values are computed first from the 6-hourly data; the yearly means are then computed from the monthly means.

Equation (2) relates the Antarctic net precipitation to the moisture transport across the Antarctic coast and the surface area of the Antarctic continent. Therefore, only the wind and moisture profiles over the ocean adjacent to the Antarctic coast are required. In this study, the Antarctic coastline is determined using the TOVS Path A data based on the geographical characteristics of the Antarctic continent. Specifically, since the Antarctic continent is mostly at elevations above 2 km, the TOVS Path A moisture at 1000 hPa is undefined. This feature is shown by the valid data percentage of the TOVS moisture at 1000 hPa (Fig. 6a). Note that the valid data percentage in Fig. 6a is computed after the temporal and spatial interpolation of the orbital satellite data onto the grid. The temporal interpolation from the orbital data to one of the four standard output UTC times reduced

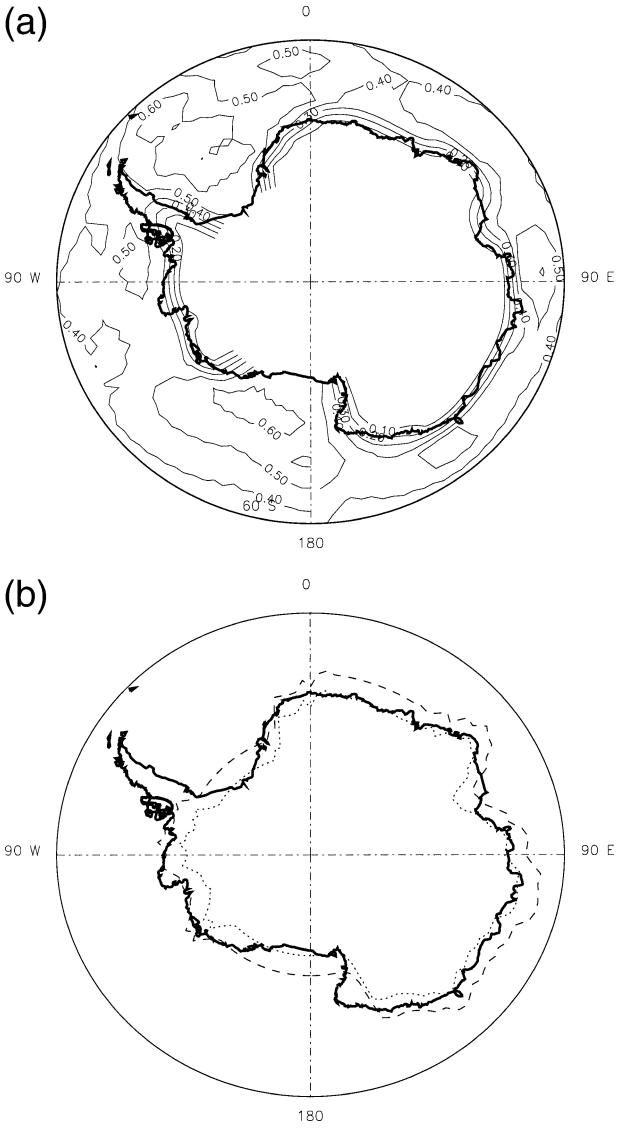

FIG. 6. (a) Contour plot of the 1988 annual mean percentage of the valid TOVS Path A moisture retrievals on the 1000-hPa level. Contour interval is 0.1. (b) The 1988 annual mean Antarctic borders obtained by the missing data method. The dotted coastline represents the 1000-hPa valid TOVS Path A moisture retrievals closest to the Antarctic missing values. The dashed coastline represents the valid moisture values 2.5° lat away from the previous dotted coastline.

the valid data percentage of the original orbital data by a factor of 4, while the spatial interpolation from 1° × 1° resolution to 2.5° × 2.5° resolution increases the valid data percentage by a factor of 6. Therefore, Fig. 6a is larger than the valid retrieval percentages of the original orbital data. However, in either case, the valid data percentage at 1000 hPa approaches zero near the Antarctic coastline. Based on this observation, the Antarctic boundary in this study is defined as the latitude of the valid 1000-hPa moisture closest to the missing continental regime. If valid data still exist poleward of 77.5°S, then 77.5°S is used as the boundary. Figure 6b shows the annually averaged Antarctic coastline (dotted line) for 1988 obtained from this approach. As seen from the figure, the shape of this border is in good agreement with the Antarctic geographic coastline; however, this border largely falls south of the Antarctic geographic coastline. Using this coastline would cause significant errors in the moisture transport estimates. Therefore, the moisture transport computation is carried out using an Antarctic border 2.5° north of this coastline. This border is represented by the dashed line in Fig. 6b. The area surrounded by this border is 15.45×10^6 km^2, equivalent to the area within the 70°S zonal circle (15.38×10^6 km^2). This area is about 10% larger than the estimated area of Antarctic continent (14×10^6 km^2; King and Turner 1997) with all islands and ice shelves included.

In order to obtain accurate estimates of the moisture transport, the wind fields must satisfy the mass balance requirement (Trenberth 1991; Bromwich et al. 1995; Cullather et al. 1998). However, because of truncation and interpolation errors, reanalysis winds may not satisfy this requirement (Trenberth 1991). Therefore, a mass balance correction for the R-2 winds must be included along the Antarctic border.

The complete mass balance equation is written as

$$\frac{\partial p_s}{\partial t} + \nabla \cdot \int_0^{p_s} \mathbf{V}\, dp = g(E - P) \tag{3}$$

(Trenberth 1991), where all the symbols have the same meanings as defined before. For observed or reanalysis data, Eq. (3) is not exactly satisfied. Using R to represent the residual term, Eq. (3) becomes

$$\frac{\partial p_s^*}{\partial t} - g(E^* - P^*) + \nabla \cdot \int_0^{p_s} \mathbf{V}^*\, dp = R, \tag{4}$$

where a star represents data from the reanalyses. Integrating (4) over the surface of the continent and dividing by the area of the continent, S, gives the spatially averaged residual. Then using Gauss's divergence theorem, one obtains the total mass flux across the closed Antarctic border

$$\frac{1}{Lp_s} \oint \int_0^{p_s} \mathbf{V}^* \cdot \mathbf{n}\, dp\, dl = -\frac{S}{Lp_s}\left[g(\langle P^* \rangle - \langle E^* \rangle) + \frac{\partial \langle p_s^* \rangle}{\partial t}\right] + \frac{S}{Lp_s}\langle R \rangle, \tag{5}$$

where we have normalized both sides of the equation with the length of the continental border, L, and the surface pressure. The left-hand side of Eq. (5) represents a vertically and coastline-averaged wind speed normal to the coast. Following Trenberth (1991), we assume that the errors exist only in the wind field and that the true wind is represented by $\mathbf{V} = \mathbf{V}^* + \mathbf{V}_c$, where $\mathbf{V}_c$ is a wind correction. Then, the sum of the surface pressure tendency, net precipitation and the true wind divergence exactly cancel, and Eqs. (4) and (5) become

$$\nabla \cdot \int_0^{p_s} \mathbf{V}_c\, dp = -R \tag{6}$$

$$\frac{1}{Lp_s} \oint \int_0^{p_s} \mathbf{V}_c \cdot \mathbf{n}\, dp\, dl = -\frac{S}{Lp_s}\langle R \rangle. \tag{7}$$

Trenberth (1991) further assumes that $\mathbf{V}_c$ is irrotational and barotropic; thus, there exists a velocity potential function, χ, such that $\mathbf{V}_c = \nabla\chi$ and Eq. (6) becomes a Poisson equation. However, solving the Poisson equation requires that χ or $\mathbf{V}_c$ be specified at the coastline as Dirichlet or Neumann boundary conditions. This is problematic since there are only limited observations at the boundary to serve as boundary conditions. To overcome the need for specifying the boundary conditions, Cullather et al. (1998) used an iterative method similar to Endlich (1967) to solve Eq. (6). However, the downside of this method is that the solution depends on specified initial-guess field (Endlich 1967).

In this study, we do not intend to solve Eq. (6) since only $\mathbf{V}_c$ on the Antarctic boundary is needed for the moisture transport computation. The vertically and coastline-averaged $\mathbf{V}_c$ on the Antarctic boundary has already been determined by Eq. (7). To see whether specific distribution of $\mathbf{V}_c$ is needed for the moisture transport computation, we split the total moisture transport by the wind correction into mean and eddy components. In particular,

$$\oint \left(\int_0^{P_s} \overline{\mathbf{V}_c q}\, \frac{dp}{g}\right) \cdot \mathbf{n}\, dl = \oint \left[\int_0^{p_s} (\overline{\mathbf{V}}_c \overline{q} + \overline{\mathbf{V}_c' q'})\, \frac{dp}{g}\right] \cdot \mathbf{n}\, dl. \tag{8}$$

Following Trenberth (1991), we assume a vertically uniform $\mathbf{V}_c$. Furthermore, it is seen from Figs. 1b and 3a that the annually averaged TPW contour lines tend to be along the Antarctic coastline near the Antarctic border for both the R-2 and TOVS Path A. Therefore, this quantity can be assumed to be a constant along the Antarctic coastline and taken out from the line integral in Eq. (8). Using Eq. (7), the mean moisture transport component in Eq. (8) becomes

TABLE 1. Comparison of the Antarctic net precipitation ($P - E$) extimates from different studies (mm yr^{-1}).

Studies	Data source	Year	Mean	Eddy	Total
Giovinetto and Bentley (1985)	Glaciological accumulation	1960–85			143
Vaughan et al. (1999)	In situ surface data	Multiyear			166
Bromwich (1990)	Glaciological $P - E$	Multiyear			151–156
Cullather et al. (1998)	ECMWF analysis $P - E$	1985–95	12	139	151
Bromwich et al. (1995)	ECMWF analysis $P - E$	1985–92			157
	NMC analysis $P - E$	1985–92			108
	ABM analysis $P - E$	1985–92			89
Bromwich et al. (1995)	ECMWF analysis $P - E$	1988			148
	NMC analysis $P - E$	1988			98
	ABM analysis $P - E$	1988			84
This study	R-2 $P - E$, equivalent Antarctic area of 70°S	1988	−11	148	137
This study	$P - E$ of TOVS/R2, equivalent Antarctic area of 70°S	1988	−7	53	46
This study	ECMWF $P - E$, equivalent Antarctic area of 70°S	1988	−21	160	139

$$\oint \left(\int_0^{p_s} \overline{\mathbf{V}}_c \overline{q} \frac{dp}{g} \right) \cdot \mathbf{n}\, dl \approx \overline{W} \oint \overline{\mathbf{V}}_c \cdot \mathbf{n}\, dl = -\frac{\overline{S}\,\overline{W}}{\overline{P}_s} \langle \overline{R} \rangle. \tag{9}$$

Equation (9) suggests that only the coastline-averaged wind correction normal to the coast is needed for evaluating the mean moisture transport.

As given in Zou and Van Woert (2001), the eddy moisture transport by the wind correction can be expressed as

$$\overline{\mathbf{V}_c' q'} = r(\mathbf{V}_c, q) \sqrt{\overline{\mathbf{V}_c'^2}} \sqrt{\overline{q'^2}}, \tag{10}$$

where $\sqrt{\overline{\mathbf{V}_c'^2}}$ represents the amplitude of the eddy wind correction and is expressed as $\sqrt{\overline{u_c'^2}}$ for the zonal, and $\sqrt{\overline{v_c'^2}}$ for the meridional component, respectively; $\sqrt{\overline{q'^2}}$ is the amplitude of the eddy specific humidity field, and $r(\mathbf{V}_c, q)$ the correlation coefficient between the wind correction and moisture fields. This correlation coefficient should be very small since there is no physical relationship between the transient wind correction and moisture fields to yield a statistically significant moisture transport. Our results indeed show that the vertically and coastline-integrated eddy moisture transport by the wind correction is nearly zero when a vertically and coastline-averaged transient wind correction is used in the computation.

In principle, given the R-2 wind, surface pressure, precipitation, and surface evaporation fields, $\langle R \rangle$ can be evaluated every 6 h using Eq. (5). However, detailed analyses suggest that only the R-2 wind data are actually needed to evaluate the residual term since the surface pressure tendency and the net precipitation terms can be ignored compared to the wind divergence term. Specifically, the computed annual mean value of the vertically and coastline-averaged R-2 wind for 1988 is 0.4 m s^{-1}. However, the long-term-averaged net precipitation over Antarctica is ~151–156 mm yr^{-1} (Bromwich 1990), corresponding to 0.4 mm day^{-1} (or about 0.001 m s^{-1} when converted to wind units). Similarly, the 1988 annual tendency of the area-averaged surface pressure over Antarctica based on R-2 is −6.7 hPa yr^{-1}, also on order of 0.001 m s^{-1} when converted to wind units. These terms are two orders of magnitude smaller than the vertically and coastline-averaged annual mean wind and therefore can be ignored in the annual mean residual computation.

In summary, the annual mean R-2 wind correction for the Antarctic border used in this study (equivalent 70°S zonal circle) for 1988 is approximately equal to the negative value of the vertically and coastline-averaged R-2 wind, that is, −0.4 m s^{-1}.

4. Results and discussion

For comparison, Table 1 lists the resulting net precipitation estimates from R-2 and the mixed TOVS moisture/R-2 wind along with other published estimates from snow stake data and model analyses. In Table 1, the multiyear glaciological data estimates suggest an Antarctic net precipitation of 151–156 mm yr^{-1} (Bromwich 1990) and a snow accumulation rate of 143 ± 14 mm yr^{-1} (Giovinetto and Bentley 1985). The most recent estimates from surface data by Vaughan et al. (1999) give an accumulation rate of 166 mm yr^{-1}, 16% higher than Giovinetto and Bentley's (1985) estimates. ECMWF analyses estimates (Cullather et al. 1998) of the long-term mean net precipitation tend to agree with the glaciological estimates within 10%. For 1988, Bromwich et al (1995) gave an ECMWF analyses estimate of 148 mm yr^{-1}, an NMC analysis estimate of 98 mm yr^{-1}, and an ABM analyses value of 84 mm yr^{-1}. These values are close to an 8-yr averaged estimate (1985 to 1992) of their corresponding analyses. The R-2 estimate in this study agrees with the ECMWF analyses estimate to within 2% for the same Antarctic coastline and agrees within 10% of the Bromwich et al. (1995) estimates for the 1988 ECMWF analyses. However, the mixed TOVS–R-2 estimate gives a substan-

tially lower value (46 mm yr^{-1}) for the total net precipitation, only 30% of the surface-based estimates.

Table 1 also shows that the mean component of the moisture convergence for R-2 and TOVS–R-2 are close to each other and that they are both small in magnitude, similar to the multiyear mean of the ECMWF analyses. Note that the listed R-2 and the mixed TOVS–R-2 mean moisture convergences are the results after application of the mass balance correction. Before the mass balance correction, the mean moisture convergence values are -63 mm yr^{-1} for R-2 and -51 mm yr^{-1} for TOVS–R-2, respectively. Therefore, the wind correction of -0.4 m s^{-1} results in a moisture convergence difference of 52 mm yr^{-1} for R-2 and 44 mm yr^{-1} for TOVS–R-2, respectively. These values are nearly 30%–35% of the total Antarctic net precipitation estimates.

This shows the significant impact of the mass balance correction on the resulting estimates of the Antarctic net precipitation. As such, potential errors may also arise from uncertainties in the assumptions used to derive the mass balance correction. For example, if the wind correction $\overline{\mathbf{V}}_c$ occurs only in the lower half of the troposphere, then the coastline-averaged wind correction would be -0.8 m s^{-1} for the lower half of the troposphere. Since more than 90% of the yearly averaged atmospheric moisture exists in the lower half of the troposphere (e.g., Peixóto and Oort 1992), the total moisture transported by the wind correction would be twice the value of the vertically uniform wind correction. Therefore, the moisture convergence difference resulting from this vertically nonuniform wind correction could be as large as ~100 mm yr^{-1}. This would substantially alter the estimated Antarctic total net precipitation and shows the importance of having an accurate annual mean wind profile. The fact that the total R-2 net precipitation estimate is close to the surface-based estimate suggests that a vertically uniform wind correction is a reasonable assumption. In addition, since the mean component of the moisture convergence is small, the large errors in the mean R-2 and TOVS Path A TPW fields discussed earlier will not have a significant impact on the results. For instance, if a 40%–50% underestimation of the mean R-2 and TOVS TPW fields near the Antarctic coast is accounted for and is assumed to be uniformly distributed in the vertical direction, it will result in a difference of ~10 mm yr^{-1} (7%) in the Antarctic net precipitation estimates.

As mentioned earlier, the mass balance correction is important only for the mean component of the moisture convergence; for the eddy component, the moisture convergence is unchanged by the mass balance correction for both the R-2 and TOVS–R-2 estimates. This occurs because the eddy moisture transport is proportional to the correlation between the wind and moisture [Eq. (10)] while the 6-hourly wind correction is physically uncorrelated with the moisture field to yield a statistically significant moisture transport.

From Table 1, we see that the R-2 eddy component dominants the total net precipitation estimates and is consistent with previous estimates based on ECMWF analyses. In contrast, the mixed TOVS–R-2 eddy component is significantly smaller than the R-2 estimate, resulting in a low total net precipitation estimate. To elucidate the reasons for the smaller eddy moisture transport of TOVS–R-2, we present a diagnostic analysis using an equation similar to Eq. (10) but with the wind correction $\mathbf{V}_c$ replaced by the R-2 meridional wind, v. This equation is evaluated using the R-2 and the mixed TOVS–R-2 data on the 60°S latitudinal circle. Figures 7a and 7b show a comparison of the 1988 annually averaged $\overline{v'q'}$ between R-2 and the mixed TOVS–R-2 products. These figures show that the R-2 data exhibit larger eddy moisture fluxes than the mixed TOVS–R-2 data, especially in the middle and upper troposphere. The vertically integrated eddy moisture convergence computed from these fluxes is 249 and 107 mm yr^{-1} for R-2 and the mixed TOVS–R-2 data, respectively. The structure of the differences at the equivalent 70°S latitude Antarctic border (Table 1) are similar; however, the percentage differences are larger.

Figures 8a and 8b show comparisons between the R-2 and TOVS Path A $\sqrt{\overline{q'^2}}$ estimates. As can be seen from the figure, in the middle and upper troposphere $\sqrt{\overline{q'^2}}$ from R-2 is 50% to 100% larger than the TOVS Path A estimates. In the earlier comparisons with the SSM/I, it was estimated that the R-2 $\sqrt{\overline{W'^2}}$ was about 40% larger than TOVS Path A value, consistent with the $\sqrt{\overline{q'^2}}$ comparisons here. The large differences in $\sqrt{\overline{q'^2}}$ partly explain the large differences in the R-2 and TOVS–R-2 $\overline{v'q'}$ estimates. Figures 9a and 9b further show the values of $r(v, q)$ for the R-2 data and the mixed TOVS–R-2 data; Fig. 9c is the ratio of Figs. 9b and 9a. Figure 9c suggests that in the lower to middle troposphere the TOVS–R-2 $r(v, q)$ is smaller than the R-2 $r(v, q)$ by 40% to 60%. The smaller correlation between the TOVS Path A moisture and R-2 wind is another important factor contributing to the small mixed TOVS–R-2 eddy moisture transport. This small correlation arises because, as found in the validation against SSM/I data, the TOVS Path A retrieves a dry (moist) atmosphere in moist (dry) conditions. In order to have a strong poleward moisture transport (larger correlation holding $\sqrt{\overline{q'^2}}$ and $\sqrt{\overline{v'^2}}$ fixed), strong poleward winds must be associated with the moist atmosphere. Since the TOVS Path A data incorrectly represent the moist and dry conditions associated with the lifting and sinking motions in baroclinic waves, strong winds will be associated with dryer than normal atmospheric conditions, leading to a lower correlation with the R-2 winds and hence, weak poleward moisture transport.

5. Conclusions

The newly released R-2 wind and moisture data as well as the TOVS Pathfinder A moisture fields have

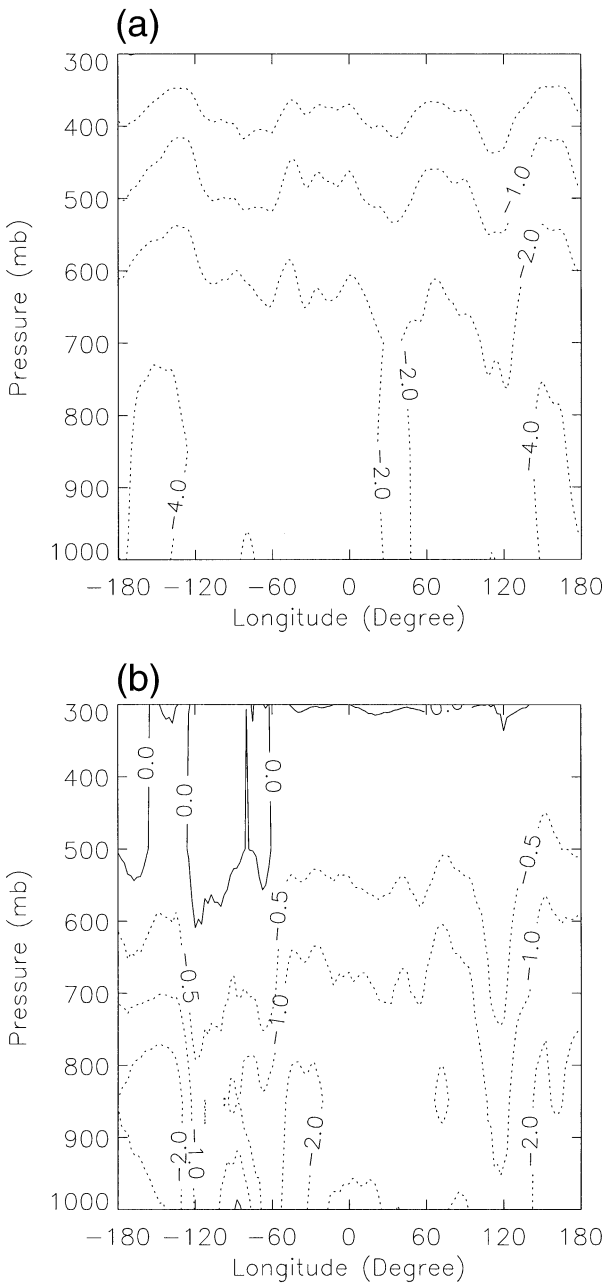

FIG. 7. The 1988 annual mean $\overline{v'q'}$ at 60°S: (a) R-2 moisture and wind, and (b) TOVS Path A moisture with the R-2 wind. Unit is m s^{-1} g kg^{-1}.

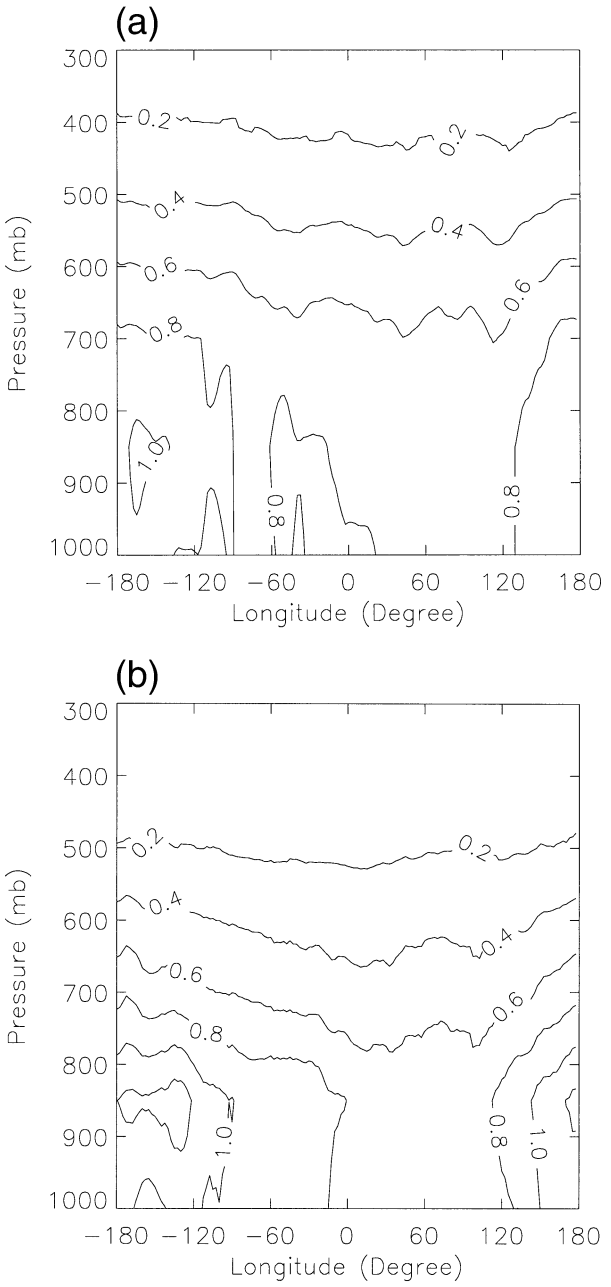

FIG. 8. The 1988 annual mean $\sqrt{\overline{q'^2}}$ at 60°S: (a) R-2, and (b) TOVS Pathfinder A. Unit is g kg^{-1}.

been examined to determine their utility for Southern Hemispheric moisture convergence estimation. A mass balance correction was applied to the R-2 wind, and then the total moisture convergence was decomposed into the mean and eddy components. It was found that the mass balance correction is important for the mean component, but can be safely ignored for the eddy component. The application of a vertically uniform wind correction appears to be a sufficient assumption for obtaining reasonable estimates of the mean moisture transport across the Antarctic coastline. The mean moisture convergence over Antarctica for the R-2 and the mixed TOVS–R-2 data were both found to be small after application of the mass balance correction, consistent with previous estimates from the ECMWF analyses. In addition, the eddy and total moisture convergence for R-2 agrees within 10% to 15% of previous ECMWF analyses estimates and surface estimates of the snow accumulation rate.

The eddy moisture convergence, and thus the total

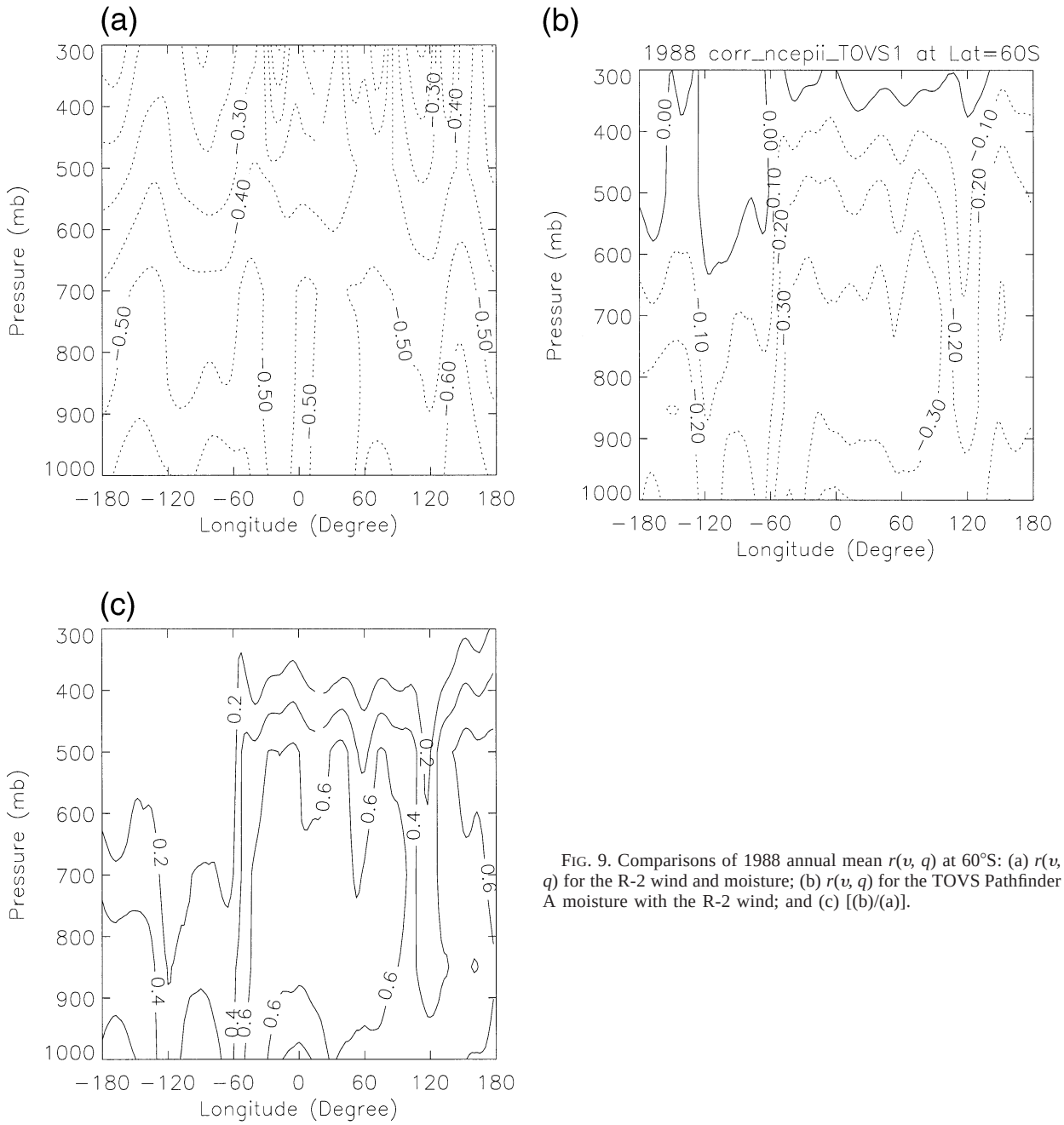

FIG. 9. Comparisons of 1988 annual mean $r(v, q)$ at 60°S: (a) $r(v, q)$ for the R-2 wind and moisture; (b) $r(v, q)$ for the TOVS Pathfinder A moisture with the R-2 wind; and (c) [(b)/(a)].

net precipitation, from the mixed TOVS–R-2 method were found to be significantly smaller than R-2 and other surface estimates. Validation and diagnostic analyses suggest that there are significant artifacts in the TOVS Pathfinder A data associated with regional atmospheric dynamics that degrade their utility for high-southern-latitude moisture budget studies. It was found that the R-2 moisture agrees quite well with the SSM/I TPW; however, the TOVS Path A moisture is almost uncorrelated with the SSM/I data. In addition, the amplitudes of the TOVS Pathfinder A eddy TPW are nearly 40% smaller than the R-2 TPW. These factors lead to an underestimation of the eddy and total moisture convergence using the mixed TOVS–R-2 method. The TOVS results presented here are specific to the Path A product, but they suggest that moisture profiles should be carefully evaluated prior to combining them with any wind product in moisture budget studies.

Acknowledgments. The NCEP–DOE Reanalysis 2 data are provided by NCAR. The authors thank David Bromwich and Jeffrey Key for their valuable comments.

The authors also thank the three anonymous reviewers whose comments greatly help the improvement of the manuscript. The views, opinions, and findings contained in this report are those of the author(s) and should not be construed as an official National Oceanic and Atmospheric Administration or U.S. government position, policy, or decision.

REFERENCES

Bromwich, D. H., 1988: Snowfall in high southern latitudes. *Rev. Geophys.,* **26,** 149–168.

——, 1990: Estimates of Antarctic precipitation. *Nature,* **343,** 627–629.

——, F. M. Robasky, R. I. Cullather, and M. L. Van Woert, 1995: The atmospheric hydrologic cycle over the Southern Ocean and Antarctica from operational numerical analyses. *Mon. Wea. Rev.,* **123,** 3518–3538.

——, A. N. Rogers, P. Kållberg, R. I. Cullather, J. W. C. White, and K. J. Kreutz, 2000: ECMWF analyses and reanalyses depiction of ENSO signal in Antarctic precipitation. *J. Climate,* **13,** 1406–1420.

Connolley, W. M., and J. C. King, 1993: Atmospheric water-vapour transport to Antarctica inferred from radiosonde data. *Quart. J. Roy. Meteor. Soc.,* **119,** 325–342.

Cullather, R. I., D. H. Bromwich, and M. L. Van Woert, 1996: Interannual variations in Antarctic precipitation related to El Niño–Southern Oscillation. *J. Geophys. Res.,* **101,** 19 109–19 118.

——, ——, and ——, 1998: Spatial and temporal variability of Antarctic precipitation from atmospheric methods. *J. Climate,* **11,** 334–367.

——, ——, and M. C. Serreze, 2000: The atmospheric hydrologic cycle over the Arctic basin from reanalyses. Part I: Computation with observations and previous studies. *J. Climate,* **13,** 923–937.

Endlich, R. M., 1967: An iterative method for altering the kinematic properties of wind fields. *J. Appl. Meteor.,* **6,** 837–844.

Francis, J. A., 1994: Improvements to TOVS retrievals over sea ice and applications to estimating Arctic energy fluxes. *J. Geophys. Res.,* **99,** 10 395–10 408.

——, 2002: Validation of reanalysis upper-level winds in the Arctic with independent rawinsonde data. *Geophys. Res. Lett.,* **29,** 1315, doi:10.1029/2001GL014578.

Genthon, C., and G. Krinner, 1998: Convergence and disposal of energy and moisture on the Antarctic polar cap from ECMWF reanalyses and forecasts. *J. Climate,* **11,** 1703–1716.

Giovinetto, M. B., and C. R. Bentley, 1985: Surface balance in ice drainage systems of Antarctica. *Antarc. J. U.S.,* **20** (4), 6–13.

——, K. Yamazaki, G. Wendler, and D. H. Bromwich, 1997: Atmospheric net transport of water vapor and latent heat across 60°S. *J. Geophys. Res.,* **102,** 11 171–11 179.

Groves, D. G., and J. A. Francis, 2002a: The moisture budget of the Arctic atmosphere from TOVS satellite data. *J. Geophys. Res.,* **107,** 4391, doi:10.1029/2001JD001191.

——, and ——, 2002b: Variability of the Arctic atmospheric moisture budget from TOVS satellite data. *J. Geophys. Res.,* **107,** 4785, doi:10.1029/2002JD002285.

Kalnay, E., and Coauthors, 1996: The NCEP/NCAR 40-Year Reanalysis Project. *Bull. Amer. Meteor. Soc.,* **77,** 437–471.

Kanamitsu, M., W. Ebisuzaki, J. Woollen, S.-K. Yang, J. J. Hnilo, M. Fiorino, and G. L. Potter, 2002: NCEP–DOE AMIP-II Reanalysis (R-2). *Bull. Amer. Meteor. Soc.,* **83,** 1631–1643.

King, J. C., and J. Turner, 1997: *Antarctic Meteorology and Climatology.* Cambridge University Press, 409 pp.

Peixóto, J. P., and A. H. Oort, 1983: The atmospheric branch of the hydrological cycle and climate. *Variations in the Global Water Budget,* A. Street-Perrott, M. Beran, and R. Ratcliffe, Eds., D. Reidel, 5–65.

——, and ——, 1992: *Physics of Climate.* American Institute of Physics, 520 pp.

Serreze, M. C., R. G. Barry, and J. E. Walsh, 1995: Atmospheric water vapor characteristics at 70°N. *J. Climate,* **8,** 719–731.

Slonaker, R. L., and M. L. Van Woert, 1999: Atmospheric moisture transport across the Southern Ocean via satellite observations. *J. Geophys. Res.,* **104,** 9229–9249.

Stephens, G. L., D. L. Jackson, and J. J. Bates, 1994: A comparison of SSM/I and TOVS column water vapor data over the global oceans. *Meteor. Atmos. Phys.,* **54,** 183–201.

Susskind, J., and J. Pfaendtner, 1989: Impact of interactive physical retrievals on NWP. *Report on the Joint ECMWF/EUMETSAT Workshop on the Use of Satellite Data in Operational Weather Prediction: 1989–1993,* Vol. 1, T. Hollingsworth, Ed., ECMWF, 245–270.

——, P. Piraino, L. Rokke, L. Iredell, and A. Mehta, 1997: Characteristics of the TOVS Path A dataset. *Bull. Amer. Meteor. Soc.,* **78,** 1449–1472.

Rogers, A. N., D. H. Bromwich, and E. H. Sinclair, 2001: The atmospheric hydrologic cycle over the Arctic basin from reanalysis. Part II: Interannual variability. *J. Climate,* **14,** 2414–2429.

Trenberth, K. E., 1991: Climate diagnostics from global analysis: Conservation of mass in ECMWF analysis. *J. Climate,* **4,** 707–722.

——, and J. G. Olson, 1988: ECMWF global analyses 1979–1986: Circulation statistics and data evaluation. NCAR Tech. Note NCAR/TN-300+STR, 94 pp.

Vaughan, D. G., J. L. Bamber, M. Giovinetto, J. Russell, and A. P. R. Cooper, 1999: Reassessment of net surface mass balance in Antarctica. *J. Climate,* **12,** 933–946.

Wentz, F., 1997: A well-calibrated ocean algorithm for Special Sensor Microwave/Imager. *J. Geophys. Res.,* **102** (C4), 8703–8718.

Zou, C.-Z., and M. L. Van Woert, 2001: The role of conservation of mass in the satellite-derived poleward moisture transport over the Southern Oceans. *J. Climate,* **14,** 997–1016.